THE ASTROPHYSICAL JOURNAL, 436:669–677, 1994 December 1

DETECTION OF EXTENDED H I ABSORPTION TOWARD PKS 2322−123 IN ABELL 2597

CHRISTOPHER P. O'DEA, STEFI A. BAUM, AND JACK F. GALLIMORE[1]
Space Telescope Science Institute,[2] 3700 San Martin Drive, Baltimore, MD 21218
Received 1994 March 11; accepted 1994 June 7

ABSTRACT

We have detected H I in absorption toward the bright radio source PKS 2322−123 associated with the central cD galaxy in the rich cluster A2597.

We detect a "narrow" velocity width component towards the nucleus which is spatially unresolved and redshifted by ~200–300 km s^{-1} from the systemic velocity. We suggest that this component may be associated with ongoing cannibalism in the cD galaxy.

We also detect a "broad" velocity width component which is spatially extended on the scale of the 3″ radio source and which is at the systemic velocity. We suggest that this component is associated with the bright Hα nebula. Our derived parameters suggest that there is much more mass in the H I than in the Hα implying that the nebula is photon bounded.

The basic observational parameters of the broad component, (e.g., systemic velocity, low optical depth, broad line width) are very similar to the absorption found in NGC 1275 (3C 84) in the Perseus cluster.

We do not detect the absorption in our very high velocity resolution data (1.5 km s^{-1}). This suggests that the H I absorption features detected in the lower resolution data are not composed of an instrumental blend and dilution of several very deep and very narrow absorption lines. Instead the broad line width and low apparent optical depth of the detected H I are apparently due to an intrinsic distribution of velocities in a population of clouds with either low covering factor $c_f < 0.05$ or low optical depth $\tau < 0.05$.

Subject headings: galaxies: clusters: individual (Abell 2597) — galaxies: elliptical and lenticular, cD — galaxies: individual (PKS 2322−123) — radio lines: galaxies

1. INTRODUCTION

Abell 2597 is thought to be a classic example of a cooling flow in a rich cluster (Crawford et al. 1989; Crawford & Fabian 1992; Heckman et al. 1989—see Table 1). The inferred mass accretion rate is $\dot{M} \sim 164\ M_\odot\ \mathrm{yr}^{-1}$ (Crawford et al. 1989; where we have scaled to our Hubble constant of 75 km s^{-1} Mpc^{-1}). The ultimate fate of the cooling gas is still an outstanding question (e.g., Fabian 1994). Over the lifetime of the cooling flow (~10^9–10^{10} yr) the accumulated gas could be as much as ~10^{11}–$10^{12}\ M_\odot$. We have undertaken a study of the "cold" component of the intracluster medium (ICM) in cooling flow clusters in order to search for clues to the fate of the cooling gas. Here we report the detection of H I in absorption against the bright radio source PKS 2322−123 in A2597.

2. OBSERVATIONS AND REDUCTION

We observed Abell 2597 with the VLA[3] (Napier, Thompson, & Ekers 1983) in A-configuration using Two-IF spectral line mode with on-line Hanning smoothing. A list of the relevant observing parameters is provided in Table 2. All observations were centered at the Doppler-shifted 21 cm line of neutral hydrogen. We obtained two sets of observations differing in bandwidth and frequency resolution: (1) a scan with a comparatively broad bandwidth ($\Delta\nu = 6.25$ MHz, $\Delta v = 1550$ km s^{-1}) and coarse resolution ($\delta\nu = 195.313$ kHz, $\delta v = 48.3$ km s^{-1}) to trace broader spectral features, and (2) three overlapping scans each with a narrow bandwidth ($\Delta\nu = 781.25$ kHz, $\Delta v = 192$ km s^{-1}) and fine resolution ($\delta\nu = 6.104$ kHz, $\delta v = 1.5$ km s^{-1}) to map narrow features which would have been diluted at the coarser resolution.

The calibration and reduction of the broadband and narrowband observations followed the same general procedure using standard routines in AIPS (see, e.g., Perley, Schwab, & Bridle 1989). Amplitude and phase calibrations were performed on the "Channel 0" data (an average of the inner 75% of the respective passbands). The Channel 0 data were edited for obviously spurious visibilities using the interactive task "TVFLG" in AIPS. The edited visibilities were then calibrated in amplitude and phase against short scans of 3C 38 ($S_\nu = 17.5$ Jy) and the nearby radio source 2243−123 ($S_\nu = 1.90$ Jy), respectively. The calibrations were refined through several iterations of self-calibration based on "CLEAN"-deconvolved models of the source. We calculated the complex bandpass response corrections based on the observations of 3C 48. Due to the poor instrumental response at the ends of the passband (two, six), frequency channels were discarded from either end of the (broadband, narrowband) visibilities.

The channel maps were prepared from the calibrated visibilities as follows. First, we subtracted the continuum emission in two steps: (1) the brighter continuum features were removed by subtracting the Fourier transform of the Channel 0 CLEAN model from the spectral line visibilities, and (2) the diffuse, residual continuum structure was next removed by averaging several channels from either end of the passband (away from any spectral features) and subtracting the result from each channel of the spectral line visibilities. "Dirty" channel maps were made by taking the Fourier transform of the edited, calibrated, and continuum-subtracted visibilities. We chose to

[1] Also at University of Maryland.
[2] Operated by the Association of Universities for Research in Astronomy, Inc., under contract with the National Aeronautics and Space Administration.
[3] The VLA is operated by the US National Radio Astronomy Observatory which is operated by Associated Universities, Inc., under cooperative agreement with the National Science Foundation.

TABLE 1

SOURCE PROPERTIES

Cluster	Abell 2597
z	0.0823
Scale (kpc arcsec^{-1})	1.4
$\dot{M}$ ($M_\odot$ yr^{-1})	164
Radio Source	PKS 2322−123
Nucleus R.A.	$23^h22^m43^s.70$
Nucleus decl.	−12°23′57″.0
Total flux density (Jy)	1.94 ± 0.04
log $P_{1.4}$ (W Hz^{-1})	25.4

NOTES.—A summary of global source properties. The redshift is from Heckman et al. 1989. The scale assumes $H_0 = 75$ km s^{-1} Mpc^{-1} and $q_0 = 0.1$. The mass accretion rate is taken from Crawford et al. 1989 and is scaled to our value of H_0. The nucleus position is taken from our VLA image and is given in 1950.0 equinox. The radio power is estimated at 1.4 GHz in the rest frame of the source.

optimize signal-to-noise over spatial resolution, so the visibilities were naturally weighted during the transform. Finally, those channel maps with strong absorption features were deconvolved using the CLEAN algorithm.

3. RESULTS

PKS 2322−123 is a small (~4–5 kpc), powerful (log $P_{1.4}$ ~ 25.4 W Hz^{-1}) radio source (Table 1 and Fig. 1) with a steep spectrum ($\alpha \sim -1.2$ near 1.4 GHz; Slee & Siegman 1983). It is thus one of the Compact Steep Spectrum radio sources (e.g., Fanti et al. 1990a, b)—though its redshift of $z = 0.082$ makes it a low-redshift example. It would be interesting to determine how many of the other CSS sources are also associated with emission line nebulae in the centers of rich clusters.

Our main result is the detection of H I in absorption against PKS 2322−123. The H I consists of two components (see Table 3 and Figs. 2, 3, and 4).

TABLE 2

OBSERVATIONAL PARAMETERS

Parameter	Value
Rest frequency (MHz)	1420.4057
Array configuration	A
Observing mode	2AD
Date of observations	1992 Nov 16
Averaging time (s)	30
Amplitude and bandpass calibrator	3C 48 (17.5 Jy)
Phase calibrator	2243−123 (1.9 Jy)
Broad Band	
Central frequency (GHz)	1.3121530 (24,703 km s^{-1})
Total bandwidth (MHz)	6.25 (1550 km s^{-1})
Final bandwidth (after editing) (km s^{-1})	1304
Spectral resolution (kHz)	195.313 (48.3 km s^{-1})
Number of spectral channels	31
Integration time (minutes)	47
Noise (rms) (mJy beam^{-1} channel^{-1})	0.83
Brightness temperature sensitivity (rms) (K)	165
Restoring beam (FWHM)	2″.32 × 1″.54 (P.A. −11°.1)
Narrow Band	
Total bandwidth (per scan) (MHz)	0.781 (192 km s^{-1})
Spectral resolution (kHz)	6.1 (1.5 km s^{-1})
Number of spectral channels	127
Combined bandpass (after editing) (km s^{-1})	524
Noise (rms) (mJy beam^{-1} channel^{-1})	6.5
Brightness temperature sensitivity (rms) (K)	823
First Scan	
Central frequency (GHz)	1.3121525 (24,703 km s^{-1})
Integration time (minutes)	14
Dirty beam (FWHM)	2″.78 × 2″.02 (P.A. −0°.76)
Second Scan	
Central frequency (GHz)	1.3128725 (24,525 km s^{-1})
Integration time (minutes)	15
Dirty beam (FWHM)	2″.84 × 2″.03 (P.A. 7°.89)
Third Scan	
Central frequency (GHz)	1.3114318 (24,881 km s^{-1})
Integration time (minutes)	15
Dirty beam (FWHM)	2″.90 × 2″.01 (P.A. 15°.6)

NOTES.—A summary of the VLA observing parameters. Values for the map noise were estimated from line-free channels. The reported velocities follow the optical convention (velocity ∝ wavelength shift) and are referenced to the heliocentric system.

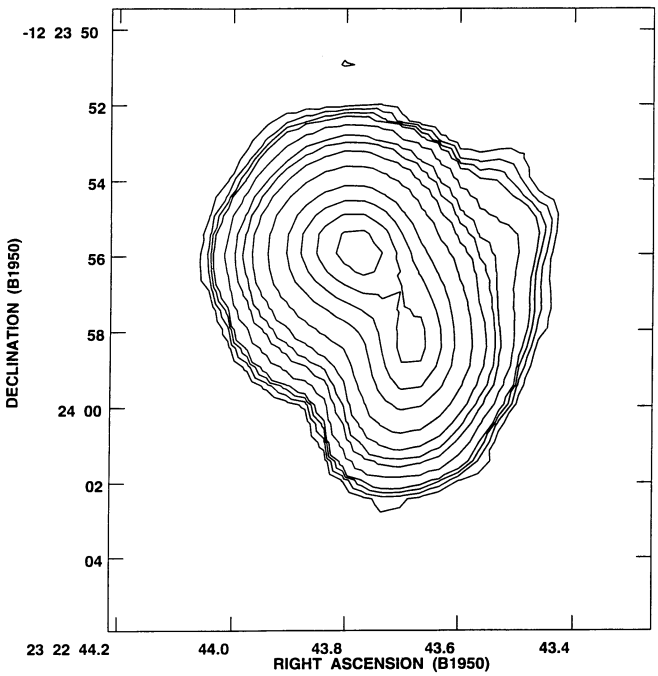

FIG. 1.—Contour plot of VLA 1.3 GHz continuum image of A2597. The contour levels are −2.0, 2.0, 3.0, 4.0, 5.0, 10.0, 20.0, 30.0, 50.0, 100.0, 200.0, 300.0, 400.0, 500.0 mJy beam^{-1}. The clean beam is 2.″3 × 1.″5 at P.A. −11°.

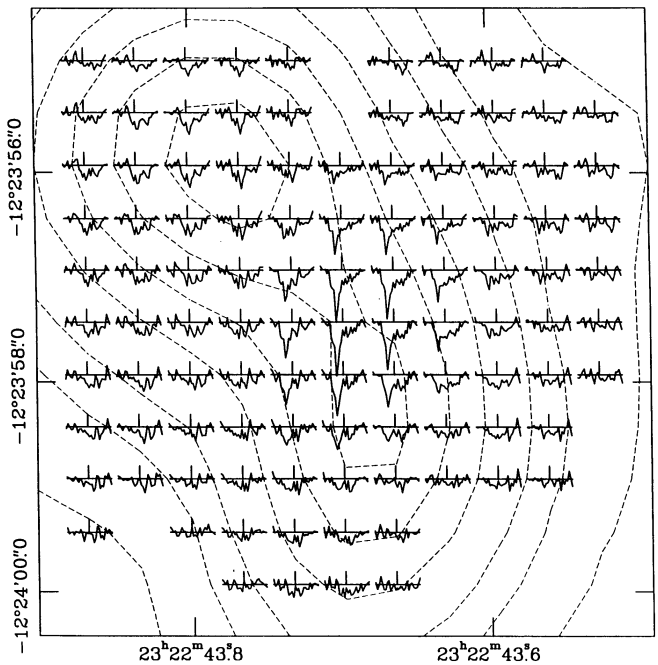

FIG. 2.—Individual H I spectra superposed on the continuum contours (*dashed lines*) of the inner portion of the VLA image (see Fig. 1). The contour levels in order of decreasing surface brightness are 500, 400, 300, 200, 100, 50, and 10 mJy beam^{-1}. Individual spectra are separated by 0.″5; the restoring beam (FWHM) covers roughly five spectra vertically and three spectra horizontally. The vertical scale bar on each spectrum is centered at 24,703 km s^{-1} and is 2.5 mJy beam^{-1} in length. Each spectrum spans 1304 km s^{-1} with velocity increasing to the left. Spectra are plotted only when the continuum-subtracted flux in three consecutive channels lies below −0.5 mJy beam^{-1}.

3.1. *The "Broad" Component*

We detect a "broad" FWHM ∼410 km s^{-1} component which is spatially resolved over the ∼3″ extent of the radio source. The central velocity is slightly blueshifted (∼70 km s^{-1}) compared to the optical redshift but given the uncertainty in the optical redshift (∼50 km s^{-1}) the broad component is consistent with being at the systemic velocity.

We note the strong similarities between the broad H I component detected in A2597 by us and in A426 (Perseus) by Crane, van der Hulst, & Haschick (1982) (see also Jaffe, De Bruyn, & Sijbreng 1988; Jaffe 1990; Sijbring 1993). The absorption lines (1) are centered at the systemic velocity, (2) have broad line widths FWHM ∼450 km s^{-1} and (3) have small apparent optical depths $\tau \sim 0.004$. Note that while the H I absorption in A2597 is spatially extended, there is yet, no confirmed evidence that the absorption feature in A426 is also extended (Sijbring 1993).

TABLE 3

H I ABSORPTION RESULTS

Parameter	Value
Broad Component	
Peak (mJy)	3.0 ± 0.3
FWHM (km s^{-1})	412 ± 40
Center velocity (heliocentric) (km s^{-1})	24604 ± 17
$\Delta S/S$	0.0056
Narrow Component	
Peak (mJy)	7.7 ± 0.3
FWHM (km s^{-1})	221 ± 10
Center velocity (heliocentric) (km s^{-1})	24886 ± 5
$\Delta S/S$	0.0187

NOTES.—A summary of the results. The peak, FWHM, and center velocity are obtained from Gaussian fits to the spectra. The parameters were determined on the nucleus for the narrow component and on the bright continuum peak to the NE of the nucleus for the broad component (where the signal-to-noise ratio is highest).

3.2. *The "Narrow" Component*

We also detect a "narrow" component with a FWHM ∼220 km s^{-1}, at the position of the nucleus which is not spatially resolved by the beam of 2.″3 × 1.″5 at P.A. = −11°. The center velocity is redshifted by 213 km s^{-1} compared to the optical velocity. The amount of the redshift could be as high as 300 km s^{-1} if the true systemic velocity is given by the center velocity of the "broad" H I component.

4. PROPERTIES OF THE DETECTED H I

The derived properties of the H I (averaged over our VLA beam) for the two components are summarized in Table 4. For distance-dependent parameters we adopt $H_0 = 75$ km s^{-1} Mpc^{-1} and $q_0 = 0.1$.

4.1. *Covering Factor*

Here we adopt the simplifying assumption that the clouds have the same covering factor at each velocity. The measured depth of the absorption line ΔS depends on both the optical depth τ and the covering factor c_f of the hydrogen,

$$\Delta S = S c_f (1 - e^{-\tau}) , \quad (1)$$

where S is the continuum flux density. This leads to expressions for the covering factor and optical depth which are not

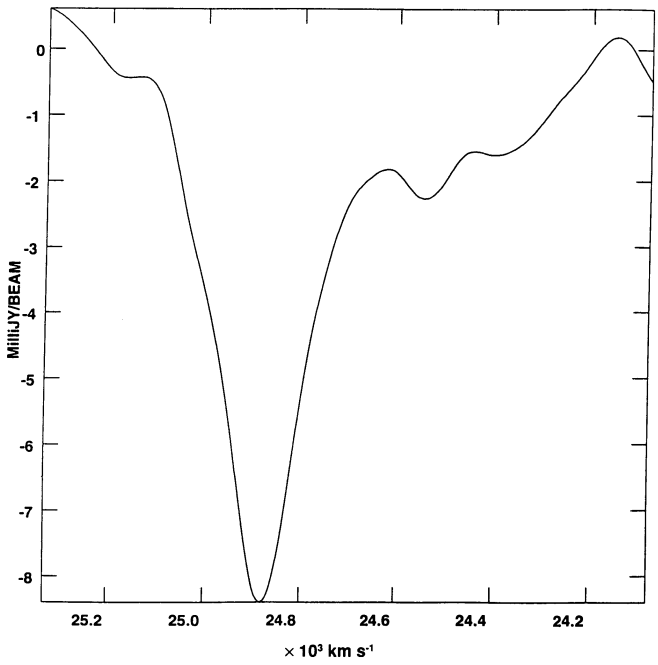

FIG. 3a

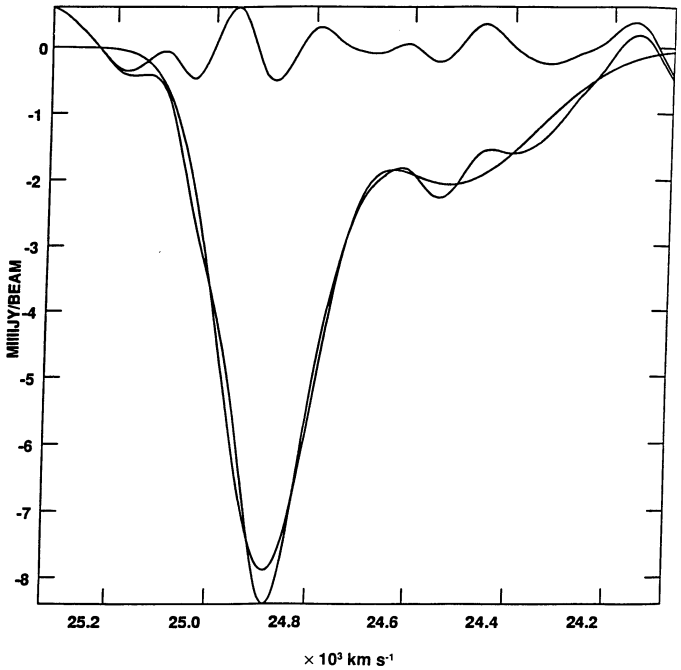

FIG. 3b

FIG. 3.—Spectrum toward the nucleus of A2597 with a 3 pixel Hanning smoothing in velocity applied. Velocity increases to the left. (*a*) The data. (*b*) The data, a two Gaussian fit, and the residuals are shown.

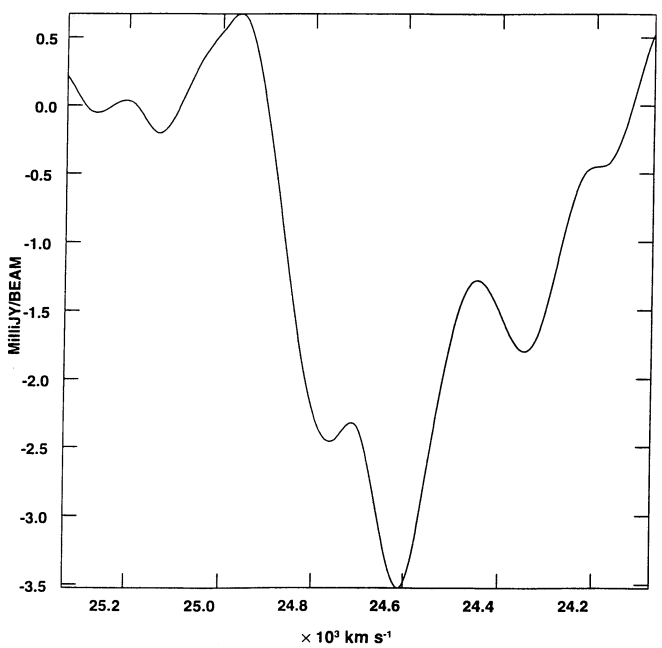

FIG. 4a

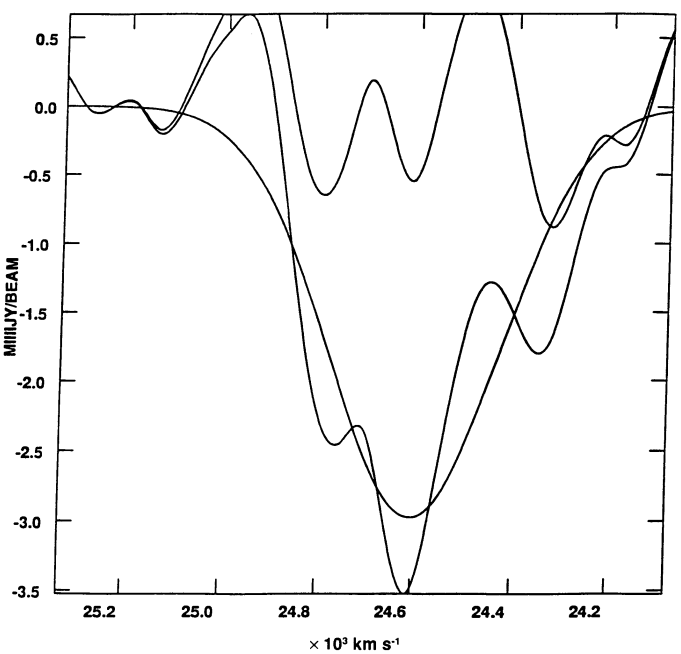

FIG. 4b

FIG. 4.—Spectrum toward the bright continuum peak of A2597, to the NE of the nucleus with a 3 pixel Hanning smoothing in velocity applied. Velocity increases to the left. (*a*) The data. (*b*) The data, a single Gaussian fit, and the residuals are shown.

TABLE 4

DERIVED PARAMETERS

Parameter	Broad Component	Narrow Component
Optical depth τ	0.006	0.019
Covering factor	$0.006 < c_f < 1$	$0.019 < c_f < 1$
Column density N_H/T_s (cm^{-2} K^{-1})	4.5×10^{18}	8.2×10^{18}
Mass M/T_s ($M_\odot$ K^{-1})	7×10^5	3.5×10^5
Cloud radius (pc)	$2.6 \times 10^{-2} < r_{cl} < 4.4$	
Number of clouds	$4 \times 10^3 < N_{cl} < 2 \times 10^{10}$	

NOTES.—A summary of the derived parameters of the H I detected in absorption. Equations, definitions, and assumptions are given in the text.

independent, (e.g., Wolfe & Burbidge 1975)

$$c_f = \frac{\Delta S}{S}(1 - e^{-\tau})^{-1}, \quad (2)$$

and

$$\tau = -\ln\left(1 - \frac{\Delta S}{S c_f}\right). \quad (3)$$

Note that (for a uniform source) there is a minimum covering factor required by the observed ratio of line depth to continuum flux density

$$c_f > \frac{\Delta S}{S} \quad (4)$$

simply because even for very large optical depth the fraction of the source flux density absorbed by the H I cannot be greater than the fraction of the source which is covered by the H I. The maximum covering factor is of course unity, so the limits on covering factor are

$$\text{Narrow: } 0.019 < c_f < 1, \quad (5)$$

$$\text{Broad: } 0.006 < c_f < 1. \quad (6)$$

4.2. *Column Density*

The column density N_H is given by

$$N_H = 1.823 \times 10^{18} T_s \int \tau \, dv \quad (7)$$

(e.g., Spitzer 1978), where T_s is the spin temperature, τ is the optical depth, and v is the velocity. If the line profile is Gaussian, then

$$N_H \simeq 1.94 \times 10^{18} T_s \tau_0 \Delta V, \quad (8)$$

where τ_0 is the peak optical depth in the line and ΔV is the FWHM of the Gaussian line profile.

The peak optical depth in the line and the FWHM are measured, however the spin temperature is not and must be estimated (see § 6). We express our values in terms of a spin temperature of 100 K, with the implicit understanding that this is uncertain.

Then, the column densities for the Narrow and Broad components are

$$\text{Narrow: } N_H \sim 8.2 \times 10^{20}\left(\frac{T_s}{100}\right) \text{cm}^{-2}, \quad (9)$$

$$\text{Broad: } N_H \sim 4.5 \times 10^{20}\left(\frac{T_s}{100}\right) \text{cm}^{-2}. \quad (10)$$

4.3. *Density*

The density of the H I is not directly measured. We assume pressure balance with ambient medium and note that the pressures inferred for the hot ICM from *ROSAT* observations (cf. Sarazin 1993, private communication), the radio source, and the Hα clouds (Heckman et al. 1989) are all in rough agreement

$$nT(\text{H}\alpha \sim \text{X-ray} \sim \text{radio}) \sim 10^6 \text{ cm}^{-3} \text{ K}. \quad (11)$$

If this is also true of the atomic gas, then $n_H \sim 10^4$ if $T_K \sim 10^2$ (see § 6).

4.4. *Mass*

The mass of the detected H I is given by $M = \pi R^2 m_H N_H$, where R is the radius of the region considered (assuming for simplicity a plane parallel geometry), and m_H is the mass of the hydrogen atom. Note that the actual mass could be higher since we only detect the gas *in front* of the radio source. The total mass depends on the radius of the distribution of H I gas. For the narrow component (which is unresolved) we use the CLEAN beam and for the broad component we use a radius of 2.5 kpc (i.e., the entire extent of the radio source). The estimated masses are

$$\text{Narrow: } M \sim 3.5 \times 10^7\left(\frac{T_s}{100}\right) M_\odot, \quad (12)$$

$$\text{Broad: } M \sim 7 \times 10^7\left(\frac{T_s}{100}\right) M_\odot. \quad (13)$$

4.5. *Kinetic Energy of the* H I

The kinetic energy in the H I clouds is given by

$$\text{KE} = (1/2) M V^2, \quad (14)$$

where V is given by $3^{1/2}\sigma$ and σ is the observed velocity dispersion of the H I. We obtain

$$\text{Narrow: KE} \sim 9.2 \times 10^{54}\left(\frac{T_s}{100}\right) \text{ergs}, \quad (15)$$

$$\text{Broad: KE} \sim 6.4 \times 10^{55}\left(\frac{T_s}{100}\right) \text{ergs}. \quad (16)$$

These estimates are conservative since we use the parameters for the H I which is *observed* in absorption against the radio source. If the broad component extends beyond (and behind) the radio source then both the mass and velocity dispersions will be larger than we have assumed here. The kinetic energy in the H I clouds is very large and thus, collisions between clouds might contribute to powering the optical emission lines in the nebula (e.g., Jaffe 1990; Baum 1992; Crawford & Fabian 1992).

The rate at which cloud collisions could conceivably supply energy to the emission lines is given by

$$L_{\rm KE} \simeq \frac{MV^3}{2r_{\rm neb}} . \quad (17)$$

We consider the inner projected $r_{\rm neb} = 2.5$ kpc of the nebula where we have H I data. We assume that a similar amount of H I exists on the far side of the radio source and that the FWHM of the H I is then 600 km s^{-1} (as given by the optical line widths). The rate at which the clouds can supply energy to the nebulae is

$$L_{\rm KE} \simeq 1 \times 10^{42} \text{ ergs s}^{-1} \frac{M}{10^8\ M_\odot} \left(\frac{V_{\rm FWHM}}{600 \text{ km s}^{-1}}\right)^3 \times \left(\frac{r_{\rm neb}}{2.5 \text{ kpc}}\right)^{-1} . \quad (18)$$

The total Hα + [N II] luminosity in this region is $\sim 10^{42}$ ergs s^{-1} (Heckman et al. 1989) which is similar to the energy input from cloud collisions. However, the Hα + [N II] is probably at most 10% of the total line emission (IR plus optical plus UV) from the nebula (e.g., Baum & Heckman 1989; Shull & McKee 1979; Kramer 1986). Thus, the kinetic energy in the clouds is probably at least an order of magnitude too low to account for the line luminosity of the nebula.

Note that we will have underestimated the mass and thus the kinetic energy in the clouds if either (1) most of the hydrogen is in molecular form (cf. Ferland, Fabian, & Johnstone 1994) or (2) the H I column density is similar over the entire extent of the optical nebulae (we can measure it only in the inner 2.5 kpc where the radio source is). If the mass of the nebula is from one to two orders of magnitude larger than we have adopted, then the kinetic energy in the nebula could supply the emission line luminosity.

5. CONSTRAINTS FROM THE HIGH-VELOCITY RESOLUTION DATA

No absorption lines were detected in the high-velocity resolution data (~ 1.5 km s^{-1}) to a 3 σ upper limit of $\tau < 0.04$ for the broad component and $\tau < 0.05$ for the narrow component. The lack of narrow lines simply suggests that the H I absorption features with broad velocity width detected in the lower resolution data are not composed of an instrumental blend and dilution of several very deep and very narrow absorption lines. This does not mean that there are no clouds with narrow line widths. From equations (2) and (3) we see that there is a range of parameter space permitted to clouds with narrow line widths. If the covering factor is of order unity, then the average optical depth must be low, $\tau < 0.05$. Conversely, if the (spatial or velocity) covering factor is low, e.g., $c_f < 0.05$ then the optical depth in clouds of narrow line width can be very high. Thus, a population of optically thick cold clouds could have escaped detection if the covering factor is low. The limits on H I absorption with narrow line widths are discussed further by O'Dea, Gallimore, & Baum (1994b) including the case where the covering factor in velocity space is much less than unity.

6. THE TEMPERATURE

6.1. *The Spin Temperature*

The astrophysics of atomic hydrogen has been considered in a series of classic papers by Field (1958, 1959a, b, c). The three processes which determine the population of the hyperfine levels in the ground state of hydrogen are (1) collisions, (2) 21 cm continuum radiation, and (3) Lα continuum radiation.

The spin temperature is given by

$$T_s = \frac{T_R + y_c T_k + y_L T_L}{1 + y_c + y_L} , \quad (19)$$

where T_R, T_k, and T_L are brightness temperature of the 21 cm continuum, the kinetic temperature, and the temperature of the Lα, respectively, and y_c and y_L are coefficients which determine the relative efficiencies of the processes.

Here we consider whether collisions or radio continuum radiation determine the population of the hyperfine levels and thus the spin temperature. We ignore the effects of the Lα continuum incident on the clouds because (1) the Lα will be destroyed by the dust which is present in the clouds (Hu 1992) and (2) the main effect of the Lα is to thermalize the hyperfine levels (Field 1959c). We have calculated the ratio of the spin temperature to the kinetic temperature for a variety of kinetic temperatures as a function of density (Fig. 5). We have used the parameterization of the collision coefficient y_c given by Bahcall & Ekers (1969). The radio source brightness temperature at a rest wavelength of 21 cm is $T_R \sim 10^5$.

Note that at low density the radio continuum raises the spin temperature, however, for densities beyond a few hundred cm^{-3} collisions dominate and thermalize the hyperfine levels bringing the spin and kinetic temperatures back into agreement. Assuming pressure balance between the H I and its ambient medium (§ 4.3) and adopting a kinetic temperature of 100 K (§ 6.2) the estimated densities are on the order of 10^4 cm^{-3} and are in the regime where the hyperfine levels are thermalized.

6.2. *The Kinetic Temperature*

Since we estimate that the hyperfine levels are thermalized by collisions and that the spin and kinetic temperatures are thus equal, it is important to estimate the kinetic temperature of the H I. We note that the following heating mechanisms are likely to be important (1) X-rays from the ICM (e.g., Donahue & Voit 1991; O'Dea et al. 1994a—see however Ferland et al. 1994) and (2) cosmic-ray protons from the radio source (e.g.,

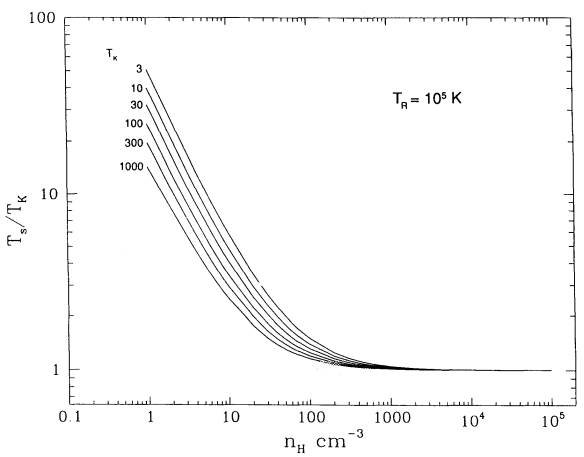

FIG. 5.—Calculation of the effects of collisions and microwave pumping (from the bright radio source) on the spin temperature of the H I in A2597 (ignoring the effect of Lα). The ratio of spin temperature to kinetic temperature is plotted as a function of hydrogen density for various values of the kinetic temperature. The radio source brightness temperature is 10^5 K.

Ferland & Mushotzky 1984; Baum & Heckman 1989; Suchkov, Allen, & Heckman 1993). As a very rough estimate, we expect the temperature of the atomic hydrogen to be in the range $T_K \sim 10^2$–10^3 K. Note that the detectability of the H I in absorption goes as

$$\tau \propto (T_s \Delta V)^{-1} \quad (20)$$

so that cooler parts of the clouds are preferentially detected. For this reason the *detected* parts of the clouds are likely to be closer to the lower end of the temperature range and we adopt $T_s = T_k \sim 10^2$ for our calculations.

7. THE ORIGIN OF THE H I

The H I we have detected in absorption must be (1) in front of PKS 2322−123 or (2) associated with A2597; however we do not know its exact location. The most likely possibilities are that the gas is (1) in the ICM of A2597 and (2) in the ISM of the central cD galaxy.

The fact that the narrow redshifted component is seen only toward the nucleus of the cD galaxy suggests that it is associated with the cD galaxy. In this case, it is most likely a spatially localized clump of gas which is falling into the nucleus of the cD. This is evidence for ongoing cannibalism in the cD. Note that evidence for infall has also been seen in some other powerful radio galaxies (van Gorkom et al. 1989).

In some clusters thought to contain cooling flows there is evidence for low-energy X-ray absorption in excess of that which would be produced by the known Galactic column density of H I (White et al. 1991; Mushotzky 1992; Allen et al. 1993). [Miyaji et al. 1993 and Wang & Stocke 1993 have also detected low energy absorption, but in clusters which are not currently thought (or known) to have cooling flows]. This has been taken to be evidence for the existence of a population of cold clouds with column density $N_H \sim 10^{21}$–10^{22} cm^{-2} and a covering factor of order unity (White et al. 1991). There is *ROSAT* PSPC data of very high quality for A2597 and the Galactic column density of H I toward this direction is very low (so it would be easy to detect excess absorption). At this point a preliminary analysis shows no evidence for such absorption (C. Sarazin 1993, private communication). Until X-ray absorbing gas is either detected or ruled out in this cluster it will not be clear whether our observations of H I have any relevance for the nature of the X-ray absorbing gas. However, searches for H I absorption in the cooling flow clusters A780, A2052, Virgo, and A2199 (Jaffe 1991; Dwarakanath, van Gorkom, & Owen 1994) would have detected H I if its properties are similar to the H I in A2597. Thus, the H I detected in A2597 must have different properties (e.g., column density, optical depth, covering factor) than the H I inferred to exist in other cooling flow clusters by White et al. (1991).

The broad component has a velocity width of $\sim$400 km s^{-1} which is similar to though somewhat smaller than the velocity width of the Hα nebula ($\sim$500–600 km s^{-1}) within the inner 10 kpc of the cD galaxy (Crawford & Fabian 1992; Heckman et al. 1989). The smaller velocity width of the H I profile is consistent with the H I absorption only sampling the line of sight in front of the radio source, while the Hα samples the entire line of sight through the nebula. Thus the broad, spatially extended H I component is *consistent* with being associated with the Hα nebula.

There is no direct one-to-one correspondence between the two absorption features detected in H I and the Hα detected in emission. However, there is no considerable "structure" in the Hα luminosity and velocity profiles, requiring the presence of multiple components (e.g., Heckman et al. 1989; Crawford & Fabian 1992). Thus, the existence of structure in the velocity profiles of the Hα is also consistent with the H I being associated with the Hα.

7.1. *The Relationship of the Detected* H I *to the Ferland et al. Clouds*

Ferland et al. (1994) consider the properties of clouds of gas heated by X-rays from the ICM. They find that the clouds have a thin ($r \sim 5.5 \times 10^{15}$ cm), warm ($T_k \sim 6000$ K) shell of atomic hydrogen with column density $N(\mathrm{H}) \sim 3 \times 10^{17}$ cm^{-2} surrounding a core of cold ($T \sim 3$ K) molecular hydrogen. Note that this result is in conflict with the results of O'Dea et al. (1994a) who estimate that X-ray heating will result in minimum equilibrium temperature in the molecular gas of $\sim$20–40 K (however, a discussion of this disagreement is beyond the scope of this paper). From equation (8) we can estimate the expected optical depth through one of these clouds assuming that the line profile would have a FWHM of 20 km s^{-1} given by the thermal width for the H I temperature of 6000 K. In this case the expected optical depth is

$$\tau = 10^{-6}\left(\frac{N_H}{10^{21}}\right)\left(\frac{\Delta V}{20\ \mathrm{km\ s^{-1}}}\right)^{-1}\left(\frac{T_s}{6000\ \mathrm{K}}\right)^{-1}. \quad (21)$$

Here $\tau \sim 10^{-6}$ and such a cloud would not be detected by these observations. It would take approximately 10^3–10^4 of these clouds along the line of sight to produce the H I absorption line detected in A2597. Such a large number of clouds along the line of sight is in general ruled out in *other* cooling flow clusters by the constraints on the velocity covering factor imposed by the sensitive limits on *warm* CO ($T \gtrsim 20$ K) as discussed by O'Dea et al. (1994). However, if the CO is very cold ($T \simeq 3$ K), then the constraints from the CO limits are not violated by having $\sim 10^3$–10^4 clouds along the line of sight and the Ferland et al. model would be consistent with the H I detection.

8. IMPLICATIONS FOR THE Hα NEBULA

Here we assume that the broad component of the H I and the Hα nebula are associated.

8.1. *Photon or Matter Bounded?*

Heckman et al. (1989) were able to determine electron densities from the [S II] λλ6717, 6731 doublet in the inner region of the nebula within a radius of 2.5 kpc. They were thus able to estimate the mass of the *ionized* nebula in this region to be $M(\mathrm{H}\alpha) \sim 6 \times 10^6\ M_\odot$. This is about an order of magnitude lower than the estimated mass of the atomic hydrogen derived in § 4.4. This suggests that the Hα nebula is photon bounded rather than matter bounded and that the Hα clouds are the ionized skins of the H I clouds. Independent evidence for substantial H I associated with the Hα nebula comes from the strong [O I] λλ6300, 6363 emission which implies a significant partially ionized zone (Heckman et al. 1989).

8.2. *Cloud Radius and Number of Clouds*

We can combine the constraint on the covering factor from the H I observations with the estimate of the volume filling factor ($v_f \sim 2 \times 10^{-5}$) from the optical observations (Heckman et al. 1989) to constrain other parameters of the

nebula, e.g., the cloud radius r_{cl} and the number of clouds N_{cl}. We assume a population of identical clouds. The covering factor and volume filling factor can be expressed as

$$c_f \simeq N_{cl} \frac{r_{cl}^2}{2r_{neb}^2}, \quad (22)$$

$$v_f = N_{cl} \frac{r_{cl}^3}{r_{neb}^3}, \quad (23)$$

where r_{neb} is the radius of the nebula (e.g., Baum 1992). The constraints on the cloud radius are then

$$r_{cl} \simeq \frac{v_f r_{neb}}{2c_f}, \quad (24)$$

which leads to

$$2.6 \times 10^{-2} \lesssim r_{cl} \lesssim 4.4 \text{ pc} \quad (25)$$

when the observational constraints are used. The constraint on the number of clouds is

$$N_{cl} \simeq \frac{(2c_f)^3}{v_f^2}, \quad (26)$$

which leads to

$$4 \times 10^3 < N_{cl} < 2 \times 10^{10}. \quad (27)$$

The parameter space is coupled such that if the covering factor is of order unity than there must be large numbers of very small clouds (i.e., $c_f = 1$, $N_{cl} \sim 10^{10}$, and $r_{cl} \sim 0.03$ pc), while if the covering factor is close to the lower limit, there must be fewer but larger clouds (i.e., $c_f = 0.006$, $N_{cl} \sim 4 \times 10^3$, and $r_{cl} \sim 4$ pc).

8.3. *The Relationship to the "Blue Lobes"*

Patches of blue light (or "blue lobes") have been found in several cooling flow radio galaxies, including A2597 (McNamara & O'Connell 1993). In A2597, the blue lobes are aligned with the radio source and in projection are essentially cospatial with it. If the H I is associated with the nebula, then it is likely that it is also cospatial with both the radio source and with the blue lobes.

Several different explanations have been proposed for the origin of the blue light (McNamara & O'Connell 1993; Crawford & Fabian 1993; Sarazin & Wise 1993). The ones which can account for the alignment with the radio source are (1) jet-induced star formation, and (2) scattering of nuclear light from a beam which escapes along the radio axis. The H I which we have detected would play a role in both cases.

In the case of jet-induced star formation, the radio jet sends shocks through clouds of cold gas in the ambient medium thereby triggering star formation (e.g., Rees 1989; Begelman & Cioffi 1989; De Young 1989; Daly 1990). In the case of scattering of nuclear light, clouds containing either dense clumps of electrons or dust scatter the light into our line of sight (Sarazin & Wise 1993). Modest amounts of dust have been inferred in the emission line filaments in A2597 by Hu (1992). Thus the existence of a population of H I clouds on the scale of the radio source and the blue lobes is consistent with *both* of these hypotheses.

9. SUMMARY

We have detected H I in absorption toward the bright radio source PKS 2322−123 associated with the central cD galaxy in the rich cluster A2597.

We detect a "narrow" velocity width component toward the nucleus which is spatially unresolved and redshifted by ~200–300 km s^{-1} from the systemic velocity. We suggest that this component is associated with ongoing cannibalism in the cD galaxy.

We also detect a "broad" velocity width component which is spatially extended on the scale of the 3″ radio source and which is at the systemic velocity. We suggest that this component is associated with the bright Hα nebula. Our derived parameters suggest that there is much more mass in the H I than in the Hα implying that the nebula is photon bounded.

The basic observational parameters of the broad component, (e.g., systemic velocity, low optical depth, broad line width) are very similar to the absorption found in NGC 1275 (3C 84) in the Perseus cluster.

We do not detect the absorption in our very high velocity resolution data (1.5 km s^{-1}). This suggests that the H I absorption features detected in the lower resolution data are not composed of an instrumental blend and dilution of several very deep and very narrow absorption lines. Instead the broad line width and low apparent optical depth of the detected H I are apparently due to an intrinsic distribution of velocities in a population of clouds with either low covering factor or low optical depth.

We find that the clouds are likely to be dense enough that the hyperfine levels are thermalized.

The existence of the H I clouds may be related to the presence of the "blue lobes" found by McNamara and O'Connell, however, it is not yet clear what the relationship is.

We are grateful to Craig Sarazin, Tim Heckman, Phil Maloney, and Andy Fabian for helpful discussions and to Carolin Crawford for useful comments on the manuscript.

REFERENCES

Allen, S. W., Fabian, A. C., Johnstone, R. M., White, D. A., Daines, S. J., Edge, A. C., & Stewart, G. C. 1993, MNRAS, 262, 901
Bahcall, J. N., & Ekers, R. D. 1969, ApJ, 157, 1055
Baum, S. A. 1992, in Proc. NATO ASI, Clusters and Superclusters of Galaxies, ed. A. C. Fabian (Dordrecht: Kluwer), 171
Baum, S. A., & Heckman, T. 1989, ApJ, 336, 702
Begelman, M. C., & Cioffi, D. F. 1989, ApJ, 345, L21
Crane, P. C., van der Hulst, J. M., & Haschik, A. D. 1982, in IAU Symp. 97, Extragalactic Radio Sources, ed. D. S. Heeschen & C. M. Wade (Dordrecht: Reidel), 307
Crawford, C. S., Arnaud, K. A., Fabian, A. C., & Johnstone, R. M. 1989, MNRAS, 236, 277
Crawford, C. S., & Fabian, A. C. 1992, MNRAS, 259, 265
———. 1993, MNRAS, 265, 431
Daly, R. A. 1990, ApJ, 355, 416
De Young, D. S. 1989, ApJ, 342, L59
Donahue, M., & Voit, G. M. 1991, ApJ, 381, 361
Dwarakanath, K. S., van Gorkom, J. H., & Owen, F. N. 1994, ApJ, 432, 469
Fabian, A. C. 1994, ARA&A, in press
Fanti, R., Fanti, C., O'Dea, C. P., & Schilizzi, R. T., eds. 1990a, Proc. Dwingeloo Workshop on Compact Steep Spectrum and GHz Peaked Spectrum Radio Sources (Bologna: Instituto di Radioastronomia)
Fanti, R., Fanti, C., Schilizzi, R. T., Spencer, R. E., Rendong, N., Parma, P., van Breugel, W., & Venturi, T. 1990b, A&A, 231, 333
Ferland, G. J., Fabian, A. C., & Johnstone, R. M. 1994, MNRAS, 266, 399
Ferland, G. J., & Mushotzky, R. F. 1984, ApJ, 286, 42
Field, G. B. 1958, Proc. I.R.E., 46, 240
———. 1959a, ApJ, 129, 525

Field, G. B. 1959b, ApJ, 129, 536
———. 1959c, ApJ, 129, 551
Heckman, T., Baum, S., van Breugel, W., & McCarthy, P. 1989, ApJ, 338, 48
Hu, E. M. 1992, ApJ, 391, 608
Jaffe, W. 1990, A&A, 240, 254
———. 1991, A&A, 250, 67
Jaffe, W. J., de Bruyn, A. G., & Sijbreng, D. 1988, in Proc. NATO ASI, Cooling Flows in Clusters and Galaxies, ed. A. C. Fabian (Dordrecht: Kluwer), 145
Kramer, S. 1986, Ph.D. thesis, Univ. Maryland
McNamara, B. R., & O'Connell, R. W. 1993, AJ, 105, 417
Miyaji, T., et al. 1993, ApJ, 419, 66
Mushotzky, R. F. 1992, in Proc. of the NATO ASI, Clusters and Superclusters of Galaxies, ed. A. C. Fabian (Dordrecht: Kluwer), 91
Napier, P. J., Thompson, A. R., & Ekers, R. D. 1983, Proc. IEEE, 71, 1295
O'Dea, C. P., Baum, S. A., Maloney, P. R., Tacconi, L. J., & Sparks, W. B. 1994a, ApJ, 422, 467
O'Dea, C. P., Gallimore, J., & Baum, S. A. 1994b, AJ, submitted
Perley, R. A., Schwab, F. R., & Bridle, A. H., eds. 1989, ASP Conf. Ser. 6, Synthesis Imaging in Radio Astronomy (San Francisco: ASP)
Rees, M. J. 1989, MNRAS, 239, 1P
Sarazin, C. L., & Wise, M. W. 1993, ApJ, 411, 55
Shull, J. M., & McKee, C. F. 1979, ApJ, 227, 131
Sijbring, L. G. 1993, Ph.D. thesis, Univ. Groningen
Slee, O. B., & Siegman, B. C. 1983, Proc. Astron. Soc. Australia, 5, 114
Spitzer, L., Jr. 1978, Physical Processes in the Interstellar Medium (New York: Wiley)
Suchkov, A., Allen, R. J., & Heckman, T. M. 1993, ApJ, 413, 542
van Gorkom, J. H., Knapp, G. R., Ekers, R. D., Ekers, D. D., Laing, R. A., & Polk, K. S. 1989, AJ, 97, 708
Wang, Q., & Stocke, J. T. 1993, ApJ, 408, 71
White, D. A., Fabian, A. C., Johnstone, R. M., Mushotzky, R. F., & Arnaud, K. A. 1991, MNRAS, 252, 72
Wolfe, A. M., & Burbidge, G. R. 1975, ApJ, 200, 548